

Integrated Sliding Mode Tracking Control of Overhead Crane Variable Reference Signal

Hesong Yuan^a, Weimin Xu

Institute of Logistics Science & Engineering, Shanghai Maritime University, Shanghai 201306, China

^a1770217105@qq.com

Abstract

An integral sliding mode control based on model reference is proposed for underactuated crane system under uncertain conditions, which not only ensures the precise positioning of trolley and the rapid load swing suppression, but also ensures the load swing in a small range and enhances safety. so that the system has a good transient response. To be specific, the sliding mode controller is designed based on the ideal reference model to generate smooth reference signals with good transient response online under different control requirements. Secondly, the integrated sliding mode controller is designed to ensure the global robustness and strong tracking performance of the system. Even in the presence of external disturbance, the bridge crane can output accurate tracking reference signal. Finally, the stability of the proposed method is proved theoretically by using Lyapunov stability, and the effectiveness of the proposed method is verified by simulation results.

Keywords

Variable Reference Signal; Overhead Crane; Moving Sliding Mode Control; Integral Sliding Mode Control.

1. Introduction

As these important and powerful transportation tools of the modern port, fast trolley positioning and small payload swing is the fundamental indices of overhead crane systems. To increase flexibility and simplify the mechanical structure, there are no direct control actions on payloads, and they have to be dragged to move toward the specified positions by the trolley translating on the girder, the number of available actuators less than degrees of freedom, and thus the overhead crane systems as typical underactuated system. Yet, compared with fully actuated systems, control of underactuated systems is much challenging [1,2]. At present, most cranes are operated by experienced workers; operation errors lead to low efficiency and serious accidents. Owing to these reasons, the study of overhead crane systems and automatic control methods has both theoretical and practical significance.

Focus on overhead crane systems, anti-swing control, transient performance and time efficiency has become a focus of the control community; various control methods have been proposed for decades [3,4]. For example, input shaping [5], trajectory planning [6], energy control [7], partial feedback control [8], fuzzy control [9], model predictive control [10], neural network control [11], optimal control [12] and other methods. The above methods can be roughly divided into open-loop control and closed-loop control. As far as open-loop control is concerned, command shaping can effectively suppress the swing angle of load. However, the problems of nonlinearity, parameter change and external disturbance in the system cannot be well dealt with. To solve this problem, a method

combining command shaping and model reference adaptive control is proposed in reference [13] to deal with the uncertainty and nonlinearity in the overhead crane system.

There are many external disturbances in the working environment of the overhead crane system, so the closed-loop control method has better control performance. In particular, sliding mode control [14,15] is widely used in controller design due to its strong robustness to the internal uncertainty of the system, simple structure and other advantages. In literature [16], nonlinear sliding mode surface is proposed. When the load mass changes, parameter uncertainties and external disturbances such as friction between trolley and beam exist in the overhead crane system, the system can still have good control performance. However, the sliding mode control have reaching stage, which is sensitive to the uncertainty and disturbance of the overhead system, affecting the transient response of the controller and leading to the decline of tracking performance. Aiming at this problem, literature [17,18,19] proposes the controller design of integrated sliding mode, which reduces the steady-state error of the system and ensures the robustness and tracking performance of the entire control system.

Although most of the above methods can achieve the load to the specified position accurately, and the swing of the load has obvious suppression and elimination. However, these methods rely on accurate mathematical model, it is very difficult for the bridge crane system. In addition, most of the control methods only consider the good anti-swing performance and stability performance, and ignore the transient response during the transmission of the overhead crane system. To solve this problem, the most direct method is to plan an appropriate trajectory for the trolley by incorporating the payload swing (caused by the trolley motion) into the trajectory planning process, and many results have been obtained [20,21,22]. In particular, in literature [23], the adaptive tracking control method is proposed to make the bridge crane transport system not only have good anti-swing performance, accelerate error convergence, and improve the transient response in the process of bridge crane transport. But how to choose a suitable path is still a problem to be solved. Model reference adaptive control stabilizes error dynamics and realizes fast dynamic response by using adaptive control law to track specific reference model signals. In literature [24], a method combining model reference adaptive with sliding mode control is proposed for the air-to-ground missile system. In the case of system parameter change and external disturbance, the actual system output tracking reference model output is made to improve the control accuracy of the system.

Therefore, this paper proposes an integrated sliding mode tracking control method with variable reference signal, which ensures that the transport load of the bridge crane system reaches the specified position under uncertain conditions and eliminates the swing angle of the load. The transient response of the system is improved. More precisely, the sliding mode controller is designed on the basis of the ideal reference model to accelerate the convergence speed of the state error of the reference model, so that the reference model can produce a smooth moving trajectory with good transient response. Then an integrated sliding mode control method is designed to speed up the output speed of the actual bridge crane system output tracking reference model and improve the robustness and tracking capability of the whole closed-loop system. The stability of the closed-loop system is proved by using Lyapunov stability and the superiority of the proposed method is verified by simulation analysis

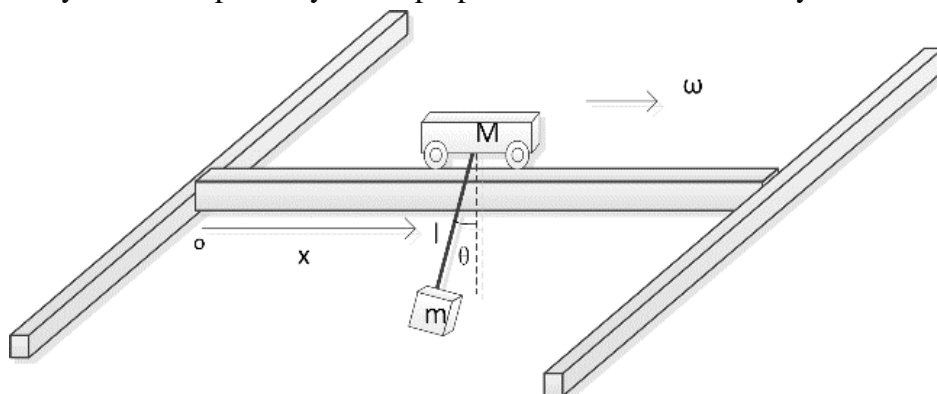


Fig.1 the model of overhead crane

2. Problem formulation

The model of the overhead crane system is shown in Figure 1, In Fig. 1, $x(t) \in \mathbb{R}$ is the trolley position, o is the starting point of the trolley. $\theta(t) \in \mathbb{R}$ denote the payload swing angle, $l \in \mathbb{R}^+$ represent the cable length, $\omega(t) \in \mathbb{R}$ is the control force imposed on trolley.

The dynamic equations, by using Lagrange’s modeling method, can be described as follows:

$$(M + m)\ddot{x} + ml\ddot{\theta} \cos \theta - ml\dot{\theta}^2 \sin \theta = \omega \tag{1}$$

$$ml^2\ddot{\theta} + ml\ddot{x} \cos \theta + mgl \sin \theta = 0 \tag{2}$$

where $M \in \mathbb{R}^+, m \in \mathbb{R}^+$ respectively representing trolley mass and the payload mass.

It can be seen from the equations (1) and (2) that the bridge crane system is a nonlinear and highly coupled underactuated mechanical system, in which an actuator is needed to control two output signals. Therefore, compared with the full drive control system, the under-drive controller designed in this paper has higher control requirements and is more difficult to realize the convergence of system errors. In order to facilitate the subsequent controller design and analysis, The dynamic equations (1)–(2) can be rewritten as

$$\begin{bmatrix} \ddot{x}_r \\ \ddot{\theta}_r \end{bmatrix} = f(x) + g(x)u_r \tag{3}$$

Where $u_r \in \mathbb{R}^{2 \times 1}$ depicts the control vector, $f(x) \in \mathbb{R}^{2 \times 1}$ represents the nonlinear system matrix, while $g(x) \in \mathbb{R}^{2 \times 2}$ denotes the input matrix. The specific definition is as follows

$$u_r = [\omega_1 \quad \omega_2]^T = \left[\omega \quad -\frac{\cos \theta}{l} \omega \right]^T \tag{4}$$

$$g(x) = \begin{bmatrix} \frac{1}{M+m \sin^2 \theta} & 0 \\ 0 & \frac{1}{M+m \sin^2 \theta} \end{bmatrix}, P = -\frac{ml\dot{\theta}^2 \sin \theta \cos \theta + mg \sin \theta \cos^2 \theta}{l(M+m \sin^2 \theta)} \tag{5}$$

However, the overhead crane system is inevitably affected by many disturbances in the actual control process of overhead crane, such as the friction between trolley and track, unmodelled system dynamics and other external disturbances. Therefore, the mathematical model described in the above formula is difficult to describe the actual bridge crane system. Considering the above factors, the actual overhead crane system is described in the following matrix form

$$\begin{bmatrix} \ddot{x} \\ \ddot{\theta} \end{bmatrix} = f(x) + \Delta f(x) + g(x)u + \Delta g(x)u + d \tag{6}$$

Where $\Delta f(x), \Delta g(x)$ model parameter variation, $d = [d_1 \quad d_2]^T$ denote the external disturbances, d_1 mainly including the friction force and other external disturbance, d_2 denotes disturbance on the load. In order to facilitate the subsequent controller design, Formula (3) is taken as the reference model and Formula (6) as the actual bridge crane model.

The control objective of this paper is to drive the output of the actual bridge crane to track the output of the reference model accurately, at the same time, to eliminate the swing angle of the payload in the presence of a series of unknown friction and uncertain disturbances. This control objective can be mathematically quantified as follows

$$\lim_{t \rightarrow \infty} x = x_r \rightarrow x_d, \lim_{t \rightarrow \infty} \theta = \theta_r \rightarrow 0 \tag{7}$$

where x_d is the expected value of the position, and x_r, θ_r is the outputs of the reference model.

3. Controller design for overhead cranes

In order to obtain the controller object in (7), the state variable errors are defined as

$$e_m = \begin{bmatrix} e_{m1} \\ e_{m2} \end{bmatrix} = \begin{bmatrix} x_r - x_d \\ \theta_r - \theta_d \end{bmatrix} \tag{8}$$

$$e = \begin{bmatrix} e_1 \\ e_2 \end{bmatrix} = \begin{bmatrix} x - x_r \\ \theta - \theta_r \end{bmatrix} \tag{9}$$

3.1 Sliding mode controller for reference model

Firstly, the smooth reference trajectory is obtained by using the reference model and sliding mode control theory. For the error signal defined in Equation (8), the sliding mode surface is designed as follows

$$s = c_m e_m + \dot{e}_m \tag{10}$$

Here $c_m = \text{diag}\{c_{m1}, c_{m2}\}$ are related to the convergence speed of the position error and swing angle error respectively. In addition, the reaching rate is used to design the controller to improve the dynamic quality of the overhead crane system. The reaching rate is as follows

$$\dot{s} = -k_{m1}s - k_{m2} \text{sgn}(s) \tag{11}$$

where $k_{m1} = \text{diag}\{k_{m11}, k_{m12}\}$, $k_{m1j} (j = 1,2)$ are switching gains; the larger the k_{m2j} , the stronger the ability to suppress the disturbances, but it will also bring about a larger chattering problem.

Finally, the driving force $\omega(t)$ can be obtained

$$\omega = g^{-1}(x)[-k_{m1}s - k_{m2} \text{sgn}(s) - c_m \dot{e}_m - f(x)] \tag{12}$$

The output signal of the reference model is

$$\ddot{x}_r = \ddot{x}_d - k_{m1}s - k_{m2} \text{sgn}(s) - c_m \dot{e}_m \tag{13}$$

Remark1: The design of the sliding mode controller in formula (12) above can ensure the asymptotic convergence of the error in the reference model is 0 and the stability of the controller can be guaranteed. However, the slope of the sliding mode surface is fixed, the slope selection is inappropriate, the time for the system to reach the sliding mode surface increases [25], and the error convergence speed is slow. This makes the time for the reference signal from the reference model to reach the expected value longer and reduces the control performance.

3.2 Time-varying reference signals

Motivated by the desire to improve the robustness of the crane system and shorten the convergence time of the crane system state errors, we propose a time-varying sliding mode surface design. The slope of the sliding mode surface is changed according to the error and velocity error, improving the transient response of the reference signal. The concrete sliding surface is designed as follows

$$\begin{aligned} s_m &= c_{m1}e_{m1} + \dot{e}_{m1} + c_{m2}e_{m2} + \dot{e}_{m2} + ae^{-bt} \\ c_{m1} &= \chi_1 \sinh\left(-\chi_2\left(\frac{e_{mi}}{\dot{e}_{mi}}\right)\right) + c_0 \\ c_{m2} &= \chi_3 \sinh\left(-\chi_4\left(\frac{e_{mi}}{\dot{e}_{mi}}\right)\right) + c_0 \\ s_0 &= c_{m1}(0)e_{m1}(0) + c_{m2}(0)e_{m2}(0) + a = 0 \end{aligned} \tag{14}$$

where c_0 is very small to ensure the slope is always positive. b is related to speed of the sliding mode surface converging to zero, $\chi_k > 0, k = 1,2,3,4$ are mainly used to decide the range and speed of the slope changing.

According to Equation (12) and (13), it can be seen that the unavoidable existence of switching functions in the reference signal and control law is likely to cause chattering phenomenon. In order to obtain smooth reference signal and suppress chattering, the super-twisting algorithm can be used to obtain the reference signal

$$\begin{aligned} \ddot{x}_r &= \ddot{x}_d - c_{m1}\dot{e}_{m1} - \dot{c}_{m1}e_{m1} - c_{m2}\dot{e}_{m2} - \dot{c}_{m2}e_{m2} - \ddot{e}_{m2} - abe^{-bt} - k_1|s_m|^{0.5} \text{sgn}(s_m) - z \\ \dot{z} &= k_2 \text{sgn}(s_m) \end{aligned} \tag{15}$$

where $k_1 > 0, k_2 > 0$ represent positive tuning parameters

According to Equations (1) and (15), the control law of the reference model can be obtained as follows:

$$\omega = (M + m)\ddot{x}_r + ml\ddot{\theta} \cos \theta - ml\dot{\theta}^2 \sin \theta \tag{16}$$

3.3 Integrated sliding mode control for tracking reference signals

This section makes the output of the bridge crane system track the reference signal accurately under the condition of the internal uncertainty and external disturbances. To achieve this goal, integrated sliding mode controller is designed to track the reference signals of the trolley and the load. Due to the coupling characteristics of the bridge crane system, according to the reference signal (15) and formula (2), the reference signal of load can be obtained as follows

$$\ddot{\theta}_r = -\frac{\cos\theta}{l}\ddot{x}_r - \frac{g}{l}\sin\theta, y_r = [x_r \ \theta_r]^T \tag{17}$$

In order to facilitate the controller design and analysis, the output of the reference model is defined as y_r . In order to eliminate the error between the output of the actual bridge crane system and the output of the reference model, the error convergence speed and tracking accuracy of the closed-loop system and the robustness of the system to external disturbances are guaranteed. The integral sliding surface design is as follows

$$\sigma = c_1 e + \dot{e} + k_c \int_0^t s_1(\tau) d\tau, s_1 = \left[e_1^{\frac{q_1}{p_1}} \ e_2^{\frac{q_2}{p_2}} \right]^T, \sigma(0) = 0 \tag{18}$$

Where $c_1 = \text{diag}\{c_{11}, c_{22}\}, k_c = \text{diag}\{k_{c1}, k_{c2}\}$ are the positive gain matrix of the controller, $c_{1j} (j = 1, 2)$ are related to the speed of eliminating the model error. $k_{cj} (j = 1, 2)$ are related to the time of error convergence. p_1, q_1, p_2, q_2 are positive odd, the ratio also determines the convergence speed of the error. The smaller the ratio, the shorter the convergence time of the error. The integral term not only makes the system always start in sliding mode, but also ensures the global robustness of the system, accelerates the convergence speed of system errors, and ensures that the system can track the output of reference model quickly and accurately. The derivative of formula (18) is obtained

$$\begin{aligned} \dot{\sigma} &= c_1 \dot{e} + \ddot{e} + k_c s_1 = \varphi(x, e) + \Delta f(x) + g(x)u + \Delta g(x)u + d \\ \varphi(x, e) &= f(x) - \ddot{y}_r + c_1 e + k_c s_1 \end{aligned} \tag{19}$$

we can obtain the control laws

$$\begin{aligned} u &= u_{eq} + u_{sw}, \quad u_{eq} = -g^{-1}(x)\varphi(x) \\ u_{sw} &= -g^{-1}(x)[k_3\sigma + (k_4 + k_5(\Phi(x, e)))\text{sgn}(\sigma)] \end{aligned} \tag{20}$$

Where $k_i = \text{diag}\{k_{i1}, k_{i2}\} (i = 3, 4, 5)$ k_{i1}, k_{i2} are the positive gain coefficient, which is used to ensure the rapid response of the system and to compensate the external disturbance. $\Phi(x, e) = \text{diag}\{|\varphi_1(x, e)|, |\varphi_2(x, e)|\}$ is additional item designed to maintain the stability.

4. Stability analysis

In order to ensure the stability of the whole closed-loop system and the actual output of the bridge crane model accurately track the output of the reference model, that is, to achieve the control goal of (7). The stability proof is divided into the following two parts.

4.1 Reference model stability analysis

Theorem 1: Considering the reference model described in Equation (3), if the slope of the sliding mode surface is updated by Equation (14), the proposed SMC law in Equation (16) can make the system state errors in Equation (8) asymptotically converge to zero, that is, $x_r \otimes x_d, \theta_r \rightarrow 0$ as time approaches infinite.

Proof: a non-negative function is selected as $V_1 = \frac{1}{2} s_m^T s_m$, differentiating it with respect to time

$$\dot{V}_1 = s_m [c_m \dot{e}_m + \dot{c}_m e_m + \ddot{e}_m - a b e^{-bt}] \tag{21}$$

Substitute Equation (8) into equation (21), and then substitute equation (3)(4) and (5) into formula

$$\dot{V}_1 = s_m [c_m \dot{e}_m + \dot{c}_m e_m + f(x) + g(x)\omega - a b e^{-bt}] \tag{22}$$

Substituting the control law (16) into equation (22), it can be obtained

$$\begin{aligned} \dot{V}_1 &= s_m[-k_1|s_m|^{0.5} \operatorname{sgn}(s_m) - z] \\ &\leq -k_1|s_m|^{0.5} s_m \operatorname{sgn}(s_m) - s_m \int k_2|s_m| \operatorname{sgn}(s_m) < 0 \end{aligned} \tag{23}$$

From the above equation, it can be seen that the moving sliding mode function will converge to 0 in finite time. According to the design of sliding mode function (14), it is not difficult to see that the error will also converge to 0 asymptotically.

4.2 Stability analysis of closed-loop control system

Theorem 3: Considering the overhead crane dynamics described in Equation (6), The proposed control laws (20) guarantee precise trolley positioning and efficient swing elimination in the sense that

$$\begin{aligned} \lim_{t \rightarrow \infty} x &= x_r \rightarrow x_d \\ \lim_{t \rightarrow \infty} \theta &= \theta_r \rightarrow 0 \end{aligned}$$

under the conditio

$$k_{3j} > 0, \quad k_{4j} > \frac{a_j}{1-b_j}, \quad k_{5j} > \frac{2b_j}{1-b_j} \quad (j = 1,2) \tag{24}$$

Assumption 1. The uncertain control input matrix is shown in the following formula

$$\begin{aligned} \Delta g(x)g^{-1}(x) &= \tilde{g}(x) \\ \tilde{g}(x) &= \begin{bmatrix} \tilde{g}_1(x) \\ \tilde{g}_2(x) \end{bmatrix} = \begin{bmatrix} g_{11} & 0 \\ 0 & g_{22} \end{bmatrix} \\ \max(|g_{1,1}|, |g_{2,2}|) &< b_j (j = 1,2), 0 < b_j < 1 \end{aligned}$$

Assumption 2 Due to actual physical limitations, it is assumed that external disturbances are bounded by internal uncertainties.

$$\|\Delta f_j(x) + d_j\| < a_j (j = 1,2)$$

Where, $\Delta f_j, d_j$ respectively represent the row of $\Delta f(x), \Delta g(x)$ in Equation (6)

Proof: A non-negative function is selected as $V_2 = \frac{1}{2} \sigma^T \sigma$, differentiating it with respect to time

$$\begin{aligned} \dot{V}_2 &= \sigma^T [\varphi(x) + \Delta f(x) + g(x)u + \Delta g(x)u + d] \\ &= \sigma^T [\Delta f(x) + d - k_3 \sigma - (k_4 + k_5(\Phi(x))) \operatorname{sgn}(\sigma) \\ &\quad - \Delta g(x)g^{-1}(x) * (\varphi(x) + k_3 \sigma + (k_4 + k_5(\Phi(x))) \operatorname{sgn}(\sigma))] \\ &= [\Delta f(x) + d - \Delta g(x)g^{-1}(x)\varphi(x)]\sigma^T - k_3[A - \Delta g(x)g^{-1}(x)]\sigma^2 \\ &\quad - (k_4 + k_5(\Phi(x)))[A - \Delta g(x)g^{-1}(x)]|\sigma| \\ &= [\Delta f_j(x) + d_j - \tilde{g}_j(x)\varphi_j(x)]\sigma_j^T - k_{3j}[A_j - \tilde{g}_j(x)]\sigma_j^2 \\ &\quad - (k_{4j} + k_{5j}(\Phi_j(x)))[A_j - \tilde{g}_j(x)]|\sigma_j| \end{aligned} \tag{25}$$

$$A = \operatorname{diag}(1,1)$$

Based on Assumption 1 and Assumption 2 can be obtained

$$\begin{aligned} \dot{V}_2 &< (a + 2b_j|\Phi_j(x)|)|\sigma_j| - k_{3j}(1 - b_j)\sigma_j^2 - (k_{4j} + k_{5j}|\Phi_j(x)|)(1 - b_j)|\sigma_j| \\ &= (a - k_{4j} + k_{4j}b_j)|\sigma_j| - k_{3j}(1 - b_j)\sigma_j^2 + (2b_j - k_{5j} + k_{5j}b_j)|\Phi_j(x)||\sigma_j| \end{aligned} \tag{26}$$

When the condition (24) is satisfied, $\dot{V}_2 < 0$ can be obtained. Barbara's lemma is easy to figure out $\lim_{t \rightarrow \infty} \sigma = 0, \lim_{t \rightarrow \infty} \theta = 0$. To sum up, theorem 2 is proved.

5. Simulations and discussion

In this section, in order to verify the applicability and effectiveness of the proposed integrated sliding mode tracking control based on the bridge crane model, some simulation studies are carried out.

Therefore, the simulation experiment is divided into two groups. In the first group, in order to prove the performance advantages of the method proposed in this paper, simulation experiments were carried out on the bridge crane model compared with those in literature [22] using the nonlinear tracking controller of fixed S-type reference signal and the controller tracking the reference signal generated by fixed sliding mode and reference model. In the second set of simulation experiments, the robustness of the controller is verified under the conditions of internal parameter change, expected value change and external disturbances.

Simulation 1. the parameters of the bridge crane system are configured as follows

$$M=6.5\text{kg}, m = 1\text{kg}, l = 1\text{m}, g = 9.8\text{m/s}^2$$

The initial values and expected values are configured as

$$x(0) = \dot{x}(0) = 0, \theta(0) = \dot{\theta}(0) = 0 \\ x_d = 0.6\text{m}, \theta_d = 0$$

In order to ensure the fairness of the comparison results, we continuously modify the gains of the three controllers in order to achieve the best control performance.

1) Nonlinear tracking of S-type reference signals [22]

$$x_r(t) = \frac{x_d}{2} + \frac{1}{2k_{22}} \ln \left[\frac{\cosh(k_{11}t - \tau)}{\cosh(k_{11}t - \tau - k_{22}x_d)} \right] \\ k_{11} = 1, k_{22} = 1, \tau = 3$$

$$F = -k_d \dot{\xi} - k_p \xi, \quad \xi = x(t) + k_1 \rho - x_r(t) \rho = \int_0^t \sin \theta \, d\tau$$

the control gains of the controller are well tuned as $k_d = 10, k_p = 4, k_1 = -2$

2) Using (20) to design the controller to trace the sliding mode to generate the reference signal

$$F = (M + m)(-\rho\sigma - \eta \operatorname{sgn} \sigma - c_{11}\dot{e}_1 - c_{22}\dot{e}_2 - \ddot{e}_2 - k_c s_1) + ml\ddot{\theta} \cos \theta - ml\dot{\theta}^2 \sin \theta$$

the control gains of the controller are $\rho = 10, \eta = 0.1, k_c = 16$

the control gains of the proposed controller are well tuned as

$$c_0 = 0.1, \chi_1 = 8, \chi_2 = 0.4, \chi_3 = 1, \chi_4 = 6, k_1 = 0.24, k_2 = 0.15 \\ k_{c1} = 12, k_{c2} = 10, c_{11} = 0.4, c_{22} = 6 \\ q_1 = 9, p_1 = 11, q_2 = 7, p_2 = 9 \\ k_3 = \operatorname{diag}\{6, 8\}, k_4 = \operatorname{diag}\{0.1, 0.3\}, k_5 = \operatorname{diag}\{1, 0.5\}$$

In order to avoid the chattering situation, the sign function in (20) is changed to the saturation function. The saturation function is expressed as follows.

$$\operatorname{sat}(\sigma_j) = \begin{cases} \frac{\sigma_j}{\zeta_j} & |\sigma_j| < \zeta_j \\ \operatorname{sign}(\sigma_j) & |\sigma_j| \geq \zeta_j \end{cases}$$

Where $\zeta_j \in (0, 1)$ is the thickness of the boundary layer of the saturation function, which determines the chattering size and the tracking error. The simulation results are shown in Figure 2

The corresponding comparison results are depicted in Fig. 2. It can be observed that the three controllers can drive both the trolley position to the desired values, but the swing angle of the payload is better suppressed and faster eliminated by the proposed controller. In addition, the proposed controller keeps the swing angle within a scope which is smaller than that of two other controllers, and there is no residual swing for the proposed controller as the trolley stops. simulation results show that the proposed controller achieves an improved control performance.

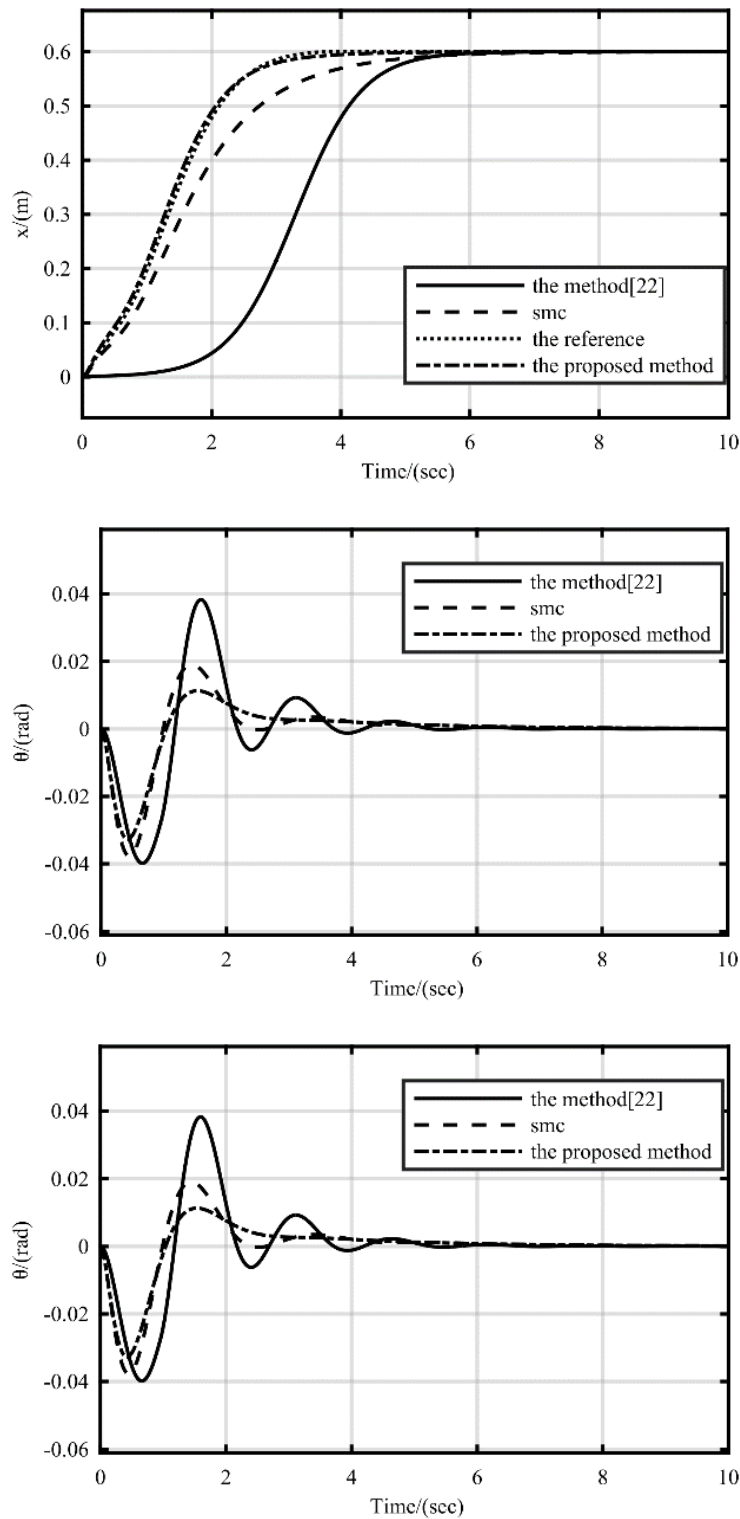


Fig.2 Compared simulation results of three control methods

Simulation 2. In the second simulation experiment, the robustness of the proposed method against external interference, internal parameter changes and expected position changes will be verified. the robustness to external disturbance and internal parameter change are verified. The parameter change of bridge crane is as follows:

$$M = 5\text{kg}, m = 0.8\text{kg}, l = 0.8\text{m}$$

External disturbances fall into the following three categories

Case1: $d_1 = D_1 = 0.5 \sin(2t)$

Case2: $d_1 = f = f_0 \tanh\left(\frac{\dot{x}}{\varpi}\right) - k_f |\dot{x}| \dot{x}$

Case3: Between 5~6s, a pulse disturbance is added to the load, and the remaining parameters are the same as Case1

Where f represents the friction in reference [16]

$$f_0 = 4.4N, \varpi = 0.01m/s, k_f = -0.5N/(m/s)^2$$

The residual parameter values remain the same as those in simulation 1. These simulation results are shown in Figure 3 below.

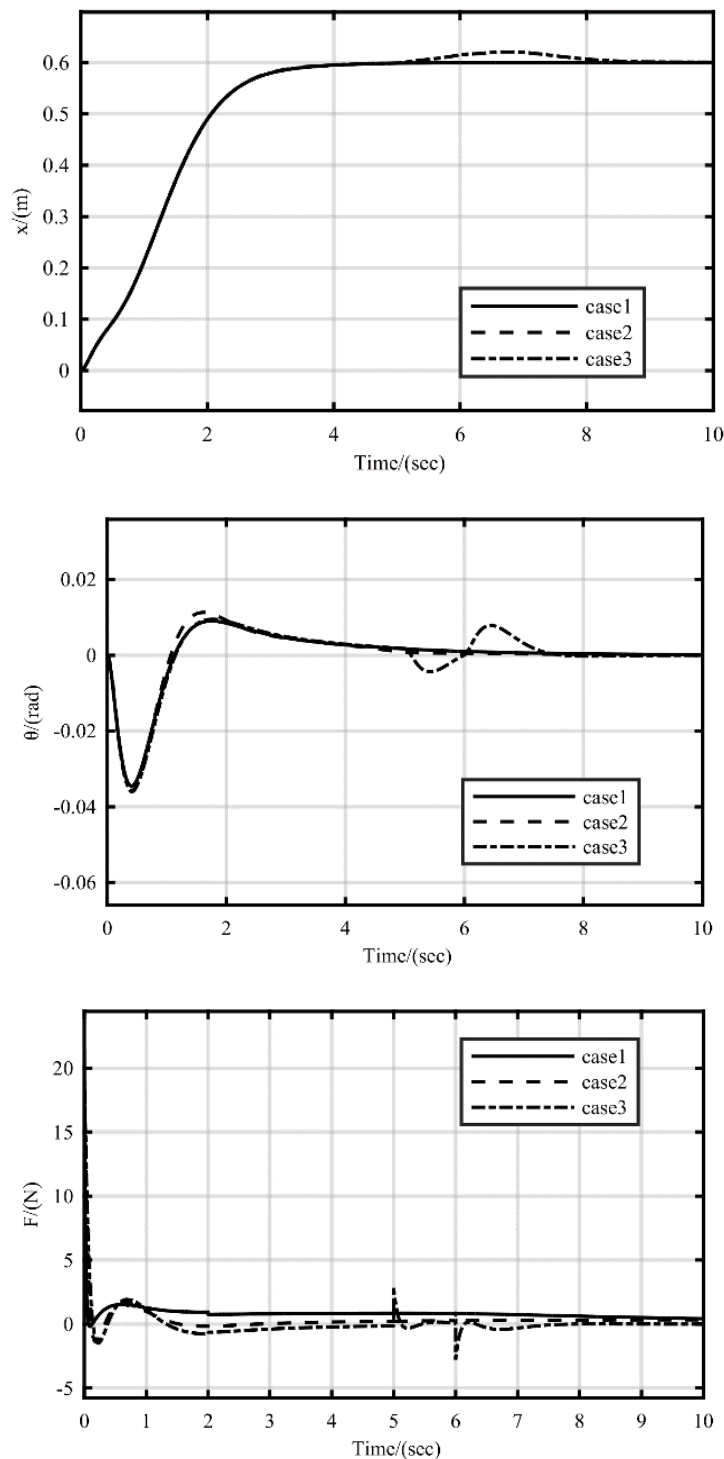


Fig. 3 Simulations with changing of parameters and different disturbances

These simulation results have evidently proven the robustness of the proposed method with respect to parameter uncertainties and external disturbances. Moreover, the proposed control method can also guarantee that the trolley tracking error is always within a prior set of boundary conditions and converges to zero rapidly.

Finally, change control objectives as follows

$$x_d = 1m, x_d = 2m$$

The remaining parameters remain unchanged in simulation 1. The simulation results are shown in Figure 4

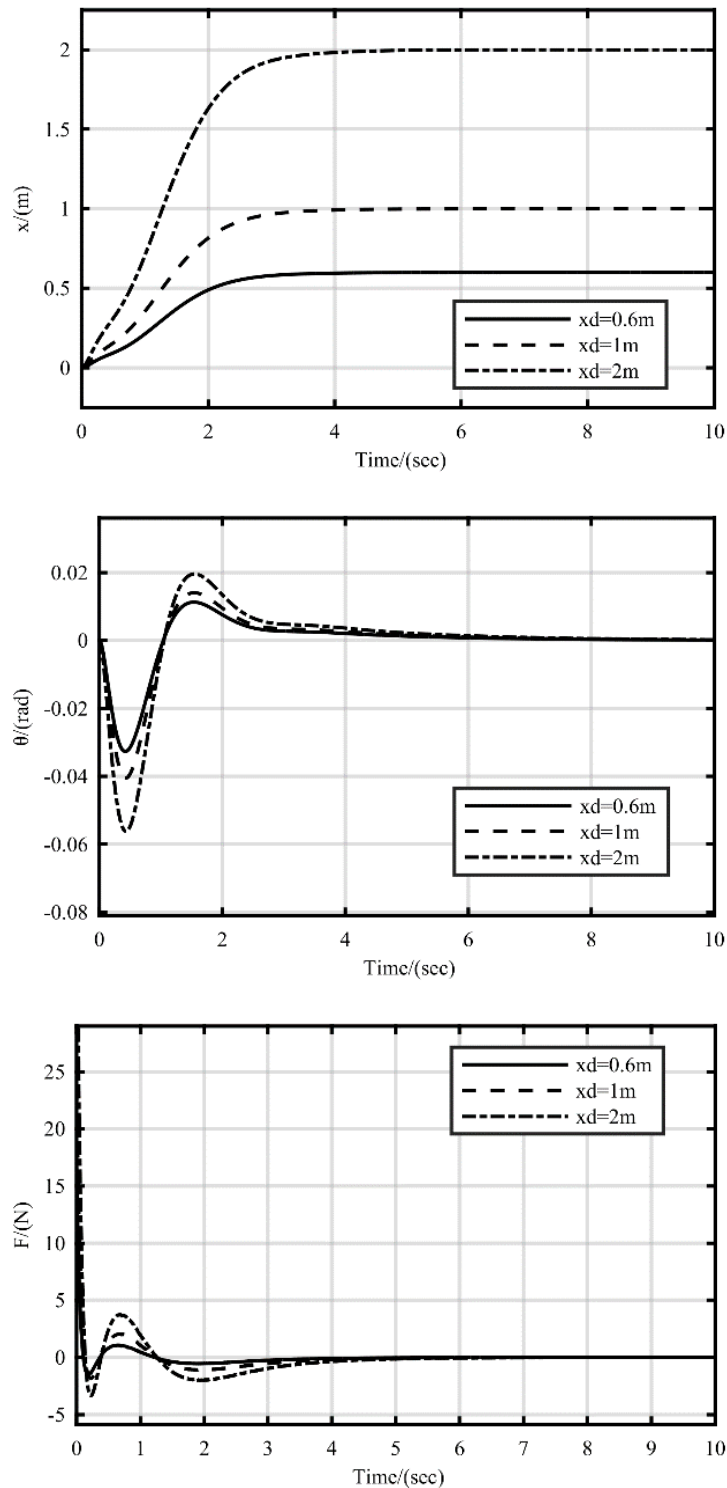


Fig.4 Comparison simulation of different expected values

By comparing the simulation results of figure 4, it can be seen that with the increase of the expected position of the trolley, the time for the trolley to reach the expected position is basically maintained at 4.5 seconds. It indicates that as the trolley speed gets faster, the load swing Angle increases. With the increase of the expected position of the trolley, the control force also increases.

Based on the above simulation experiments, it can be seen that the control method proposed in this paper can quickly realize the trolley positioning and load anti-swing while ensuring the transient response of the system. The problem of slow swing angle suppression for fixed reference signal load and difficult design of reference signal is solved. At the same time, the controller designed in this paper can guarantee the stable operation of the bridge crane and the good transient response of the system in the presence of external disturbance

6. Conclusion

This paper proposed an integral sliding mode controller for 2-D under-actuated cranes with time-varying reference signal, which achieves precise trolley positioning, with improved transient performance on swing suppression and elimination. The proposed controller and the corresponding stability analysis are derived directly from the system's original nonlinear model instead of a linearized model around the equilibrium point. Simulation results are provided to validate the effectiveness of the proposed controller. Consider input saturation in future work.

References

- [1] Tan Y, Xu W, Xu P, et al. Design of anti-sway positioning controller of overhead crane based on dynamic sliding mode structure[J]. *Control engineering*, 2013, 20(5): 117-12.
- [2] Wu X, Xu K, He X. Disturbance-observer-based nonlinear control for overhead cranes subject to uncertain disturbances[J]. *Mechanical Systems and Signal Processing*. 2020, 139: 106631.
- [3] Chen H, Fang Y, Sun N. A payload swing suppression guaranteed emergency braking method for overhead crane systems[J]. *Journal of Vibration and Control*. 2017, 24(20): 4651-4660.
- [4] Zhang M, Zhang Y, Chen H, et al. Model-independent PD-SMC method with payload swing suppression for 3D overhead crane systems[J]. *Mechanical Systems and Signal Processing*. 2019, 129: 381-393.
- [5] Maghsoudi M J, Ramli L, Sudin S, et al. Improved unity magnitude input shaping scheme for sway control of an underactuated 3D overhead crane with hoisting[J]. *Mechanical Systems and Signal Processing*. 2019, 123: 466-482.
- [6] Peng H, Shi B, Wang X, et al. Interval estimation and optimization for motion trajectory of overhead crane under uncertainty[J]. *Nonlinear Dynamics*. 2019, 96(2): 1693-1715.
- [7] Sun N, Fang Y. Nonlinear tracking control of underactuated cranes with load transferring and lowering: Theory and experimentation[J]. *Automatica*. 2014, 50(9): 2350-2357.
- [8] Wu X, He X. Partial feedback linearization control for 3-D underactuated overhead crane systems[J]. *ISA Transactions*. 2016, 65: 361-370.
- [9] Ranjbari L, Shirdel A H, Aslahi-Shahri M, et al. Designing precision fuzzy controller for load swing of an overhead crane[J]. *Neural Computing and Applications*. 2015, 26(7): 1555-1560.
- [10] Chen H, Fang Y, Sun N. A Swing Constraint Guaranteed MPC Algorithm for Underactuated Overhead Cranes[J]. *IEEE/ASME Transactions on Mechatronics*. 2016, 21(5): 2543-2555.
- [11] Ramli L, Mohamed Z, Jaafar H I. A neural network-based input shaping for swing suppression of an overhead crane under payload hoisting and mass variations[J]. *Mechanical Systems and Signal Processing*. 2018, 107: 484-501.
- [12] Wang D, He H, Liu D. Intelligent Optimal Control With Critic Learning for a Nonlinear Overhead Crane System[J]. *IEEE Transactions on Industrial Informatics*. 2018, 14(7): 2932-2940.
- [13] Jaafar H I, Mohamed Z, Shamsudin M A, et al. Model reference command shaping for vibration control of multimode flexible systems with application to a double-pendulum overhead crane[J]. *Mechanical Systems and Signal Processing*. 2019, 115: 677-695.

- [14]Zhang M, Zhang Y, Cheng X. An Enhanced Coupling PD with Sliding Mode Control Method for Underactuated Double-pendulum Overhead Crane Systems[J]. International Journal of Control, Automation and Systems. 2019, 17(6): 1579-1588.
- [15]Singh A M, Ha Q P. Fast Terminal Sliding Control Application for Second-order Underactuated Systems[J]. International Journal of Control, Automation and Systems. 2019, 17(8): 1884-1898
- [16]Liu B, Xu W, Chu J. Multi-sliding structure control of overhead crane[J]. Control engineering,2012,19:78-81.
- [17]Jiang T, Lin D, Song T. Novel integral sliding mode control for small-scale unmanned helicopters[J]. Journal of the Franklin Institute. 2019, 356(5): 2668-2689.
- [18]Qiao L, Zhang W. Double-Loop Integral Terminal Sliding Mode Tracking Control for UUVs With Adaptive Dynamic Compensation of Uncertainties and Disturbances[J]. IEEE Journal of Oceanic Engineering. 2019, 44(1): 29-53.
- [19]Li Y, Tang C, Peeta S, et al. Integral-Sliding-Mode Braking Control for a Connected Vehicle Platoon: Theory and Application[J]. IEEE Transactions on Industrial Electronics. 2019, 66(6): 4618-4628.
- [20]Zhang M, Ma X, Chai H, et al. A novel online motion planning method for double-pendulum overhead cranes[J]. Nonlinear Dynamics. 2016, 85(2): 1079-1090.
- [21]Li F, Zhang C, Sun B. A Minimum-Time Motion Online Planning Method for Underactuated Overhead Crane Systems[J]. IEEE Access. 2019, 7: 54586-54594.
- [22]Li X, Peng X, Geng Z. Anti-swing control for 2-D under-actuated cranes with load hoisting/lowering: A coupling-based approach[J]. ISA Transactions. 2019, 95: 372-378.
- [23]Zhang M, Ma X, Rong X, et al. Adaptive tracking control for double-pendulum overhead cranes subject to tracking error limitation, parametric uncertainties and external disturbances[J]. Mechanical Systems and Signal Processing. 2016, 76-77: 15-32.
- [24]Zhang L, Wei C, Rong W U, et al. Fixed-time adaptive model reference sliding mode control for an air-to-ground missile[J]. Chinese Journal of Aeronautics, 2019, 032(005):1268-1280.
- [25]çakar O, Tanyıldızı A K. Application of moving sliding mode control for a DC motor driven four-bar mechanism[J]. Advances in Mechanical Engineering. 2018, 10(3): 2072045306.